Novel catalysts expanding the temperature range for NO selective catalytic reduction by H₂

Downloaded from: https://research.chalmers.se, 2024-09-27 14:19 UTC

Citation for the original published paper (version of record):
Shao, J., Ho, H., Creaser, D. et al (2024). Novel catalysts expanding the temperature range for NO selective catalytic reduction by
H₂. APPLIED CATALYSIS O: OPEN, 188.
http://dx.doi.org/10.1016/j.apcato.2024.206947

N.B. When citing this work, cite the original published paper.

research.chalmers.se offers the possibility of retrieving research publications produced at Chalmers University of Technology. It covers all kind of research output: articles, dissertations, conference papers, reports etc. since 2004. research.chalmers.se is administrated and maintained by Chalmers Library

(article starts on next page)

188 (2024) 206947

Contents lists available at ScienceDirect

Applied Catalysis O: Open

journal homepage: www.elsevier.com/locate/apcato

Novel catalysts expanding the temperature range for NO selective catalytic reduction by H_2

Jieling Shao, Phuoc Hoang Ho, Derek Creaser, Louise Olsson *

Chemical Engineering, Chalmers University of Technology, 412 96 Gothenburg, Sweden

ARTICLE INFO

Keywords:
H_2-SCR
Temperature range
SSZ-13 zeolite
BETA zeolite
Noble metals

ABSTRACT

Nobel metal (Pt, Pd, Ir) based catalysts are developed to cover a wide working temperature window for exhaust emission control from H_2 internal combustion engines. A preliminary exploration including measurement of catalytic activities, redox states, and reaction processes is carried out regarding how the functions of the three metals varied with temperature.

1. Introduction

The EU regulations on greenhouse gas emissions and the new Euro 7 standards which are proposed to stipulate near-zero emission requirements for CO_2 and other exhaust gases pose ever greater challenges for the emission control of engine exhausts, thus the applications of hydrogen energy have been further promoted [1]. Compared to conventional diesel, H_2 has a wider range of flammability and low ignition energy demand, which means H_2-ICE can reach stable combustion at an earlier stage resulting in a shorter cold start [2]. Hydrogen gives carbon-free energy, and in principle, nitrogen oxides (NO_x) are the only undesirable engine emissions [3]. Therefore, NO_x reduction units are necessary for the after-treatment. Compared to the conventional ammonia-SCR, H_2-SCR exhibit lower activity and selectivity. However, H_2-SCR has a large advantage since it does not require a urea tank and injection system on the vehicles, which is why its development is important for the future.

Platinum group metals, in particular, Pt and Pd have been commonly proposed to have the most activity for NO_x reduction by H_2 [4–6]. Over two decades of research, many scholars have found that Pt-based catalysts could reach a high NO conversion at low temperatures (100–200 °C), however with a problematic high selectivity for the formation of N_2O, an unwanted byproduct of H_2-SCR [7]. Burch et al. found that the reduction of NO started from 40 °C and reached a maximum conversion of 75% at 90 °C on a Pt/SiO_2 catalyst [8]. Opposite to the catalyst performance of Pt-based catalysts, Pd counterparts are attractive for NO reduction with higher N_2 selectivity. A $Pd/\gamma\text{-}Al_2O_3$ catalyst showed NO conversion of over 95% and N_2 selectivity of above 80% at 200 °C [9]. Apart from Pt and Pd, Ir has been reported to offer two advantages - higher N_2 selectivity and high-temperature catalytic properties. In particular, Ir-based catalysts can still convert NO to N_2 at high temperatures (>300 °C) under an oxygen environment when the catalyst surface is dominated by oxygen [10]. It should be noted that the competitive reaction, hydrogen combustion, is highly active on the noble metals at high temperatures. Additionally, noble metals may suffer sintering and ageing at elevated temperatures [11]. Therefore, the development of catalysts working over a wide temperature range is important to not only prevent cold start emissions (low temperature) but also retain good catalytic H_2-SCR performance at medium/high temperatures (300–500 °C) [12,13].

In recent years, zeolites, have been reported to have a positive effect, especially for N_2 selectivity on H_2-SCR catalysts [7,14]. Wen et al. used MFI zeolite as a support to load Pd and achieved a NO conversion of 70% at 100 °C without any byproducts over a broad temperature range (100–400 °C) [15]. Deutschmann and co-workers modified ZSM-5 and Y zeolite by TiO_2 and compared their performance. The light-off measurements showed that Pd supported on the modified Y zeolite catalyst had a superior performance for NO conversion and N_2 selectivity than the ZSM-5-supported catalyst [16]. Chabazite - a typical small-pore zeolite, is a well-known support for the development of Cu-based catalysts for the NH_3-SCR application, which have superior activity and N_2 formation selectivity due to their extraordinary physiochemical properties and hydrothermal stability [17,18]. However, they have not been commonly used for the development of H_2-SCR catalysts. In one of few

* Corresponding author.
E-mail address: louise.olsson@chalmers.se (L. Olsson).

https://doi.org/10.1016/j.apcato.2024.206947
Received 16 February 2024; Received in revised form 1 May 2024; Accepted 23 May 2024
Available online 24 May 2024
2950-6484/© 2024 The Authors. Published by Elsevier B.V. This is an open access article under the CC BY license (http://creativecommons.org/licenses/by/4.0/).

studies, Pt/SSZ-13 was shown to exhibit an NO conversion of 81% at 100 °C with 91% selectivity for N_2 and this catalyst was better than Pt/ZSM-5 and Pt/SAPO-34 during stability tests in the presence of SO_2 and H_2O [19].

There seems to be a certain academic consensus on the performance of Pt and Pd for H_2-SCR, but interestingly there are still discrepancies in the limited studies on Ir-based catalysts. Burch et al. have reported that Ir had no activity for H_2-SCR [8]. By contrast, Nanba and co-workers have demonstrated that iridium, even though possessing lower reactivity than Pt or Pd, does exhibit definite activity [20], which is supported by DFT calculations that Ir is most active for NO reduction only at Ir (211) facet [10]. The authors concluded that the nature of the noble metals can affect the working temperature. However, this work only focused on the activity in the low-temperature region and the increased N_2 selectivity on Pt-based catalysts. It should be noted that most of the data reported in the literature until now has involved the testing of powder catalysts. Compared to these, our work is a systematic study of honeycomb monoliths containing Pt/Pd/Ir supported on SSZ-13 zeolite catalysts and focuses on both low and high-temperature performance. It is well known that monolith catalysts have different transport properties than packed beds of catalysts and are preferred for application in aftertreatment systems [21].

2. Experimental

The SSZ-13 zeolite was synthesized by a hydrothermal method. The monometallic Pt/Pd/Ir supported on SSZ-13 catalysts with 1 wt% loading (confirmed by ICP-SFMS test) was prepared by an incipient wetness impregnation method. The powder catalysts were wash-coated onto the honeycomb monoliths. The activity tests were carried out using a flow reactor with the monolith inserted. The details of the sample preparation, flow reactor setup, activity test protocol and characterization are provided in the **Supplementary Information (SI)**.

3. Results and discussion

Fig. 1 and Fig. 2 compare NO conversion, selectivities, and the amount of N_2 produced, by the three catalysts with different active noble metal elements. The NO conversion trend is Pt > Pd > Ir, and the maximum nitrogen generation reached 100 ppm, 45 ppm, and 10 ppm, respectively. Also, Fig. 2 reflects that the temperature intervals affected by the three different active centres have a clear trend from low to high, which corresponds exactly to the catalytic activity. For example, the Pt catalyst has the lowest active temperature interval (80–250 °C) for H_2-SCR and the highest reactivity. As shown in Table 1, based on XPS experiments, only the Pt catalyst was predominantly in its metallic state (73.7%) among the three catalysts. Whereas the noble metals in both Pd and Ir catalysts are in their oxidized states (Pd^{2+}/Pd^{4+} and Ir^{3+}/Ir^{4+}, respectively). Hence, the redox state is different for the three samples and could be one of the reasons for the differences in reactivity. The reduction of NO to N_2 on the Pd catalyst occurs at a higher and wider temperature interval (110–390 °C) than for Pt/SSZ-13. However, NO conversion is relatively low compared to Pt (Fig. 1), and the maximum amount of N_2 production is approximately 45 ppm. It is noticed that the Pd catalyst shows a maximum N_2 selectivity of about 80% within its active temperature range. This selectivity for N_2 is greater than the maximum selectivity of 75% of the Pt catalyst that only exists at a certain temperature point.

The nature of Pt and Pd differed in their activity for H_2 oxidation, also Pt/SSZ-13 existed in a more metallic state than the Pd sample, resulting in faster H_2 consumption by its combustion which is shown in **Fig. S1**. Unlike Pt and Pd, the NO reduction performance of the Ir catalyst was near negligible after the degreening pretreatment (Fig. 1 and Fig. 2). However, the catalytic performance of the Ir catalyst increased after the H_2 pretreatment. Surprisingly, the Ir catalyst could reduce NO to N_2 at temperatures beyond 300 °C with only a small formation of N_2O and NO_2. The ability of the Ir catalyst to catalyse NO reduction at a high-temperature range is related to the nature of Ir. This is shown by the fact that Ir had the least low-temperature activity for H_2 oxidation (**Fig. S1**) and therefore the H_2 oxidation was not equally competitive with H_2-SCR of NO, unlike the case with the Pt catalyst. Thus, the different temperature characteristics of the three catalysts were related to the characteristics of the oxidation reaction of hydrogen over the catalysts. Li et al. have investigated the H_2 oxidation performance on an O_2-rich IrO_2 surface. They observed that H_2 can be efficiently dissociated on the IrO_2 (110) surface, but that H_2O desorption is the limiting step suppressing the H_2O production [22]. This would suggest that the activity of the Ir catalyst may be strongly inhibited by the 5% H_2O in the feed at low temperatures. Both slower competitive hydrogen combustion and the more inert nature of iridium are reasons why H_2-SCR occurs at high temperatures.

Since each catalyst exhibited distinct working temperature windows, an attempt was made to examine the activity of a combination of the three catalysts positioned sequentially in order of Ir/SSZ-13-Pd/SSZ-13-Pt/SSZ-13, while maintaining the same space velocity and feed gas composition. The catalyst series was arranged with Pt positioned furthest downstream to avoid premature hydrogen consumption, since it is highly active in hydrogen combustion, as observed in **Fig. S1**. The Pd catalyst was placed in the middle and Ir was the first catalyst. Note that pre-oxidized (de-greened) catalysts were used. The formation of N_2 product from the H_2-SCR of NO was detected by a mass spectrometer because N_2 is not detectable by FTIR analysis. Fig. 3(a) shows that nitrogen generation in the activity test exhibits two distinct peaks for the lower and middle-temperature ranges. Since pre-oxidized iridium catalyst activity was inherently low,it had a neglectable activity in this experiment and there is no clear peak at higher temperature.

In view of the special high temperature NO reduction, but low activity of the Ir catalyst, a reduction pretreatment was investigated as a strategy to improve its reactivity. It is surprisingly observed in Fig. 2, that the N_2 formation was approximately doubled with the reduction pretreatment. However, when examining the N_2 generation as well as the water generation data for repeated cycles of H_2-SCR over the

Table 1
X-ray photoelectron data including redox states, binding energy, and state fractions de-greened 1 wt% Pt, Pd, Ir/SSZ-13, 1 wt% Ir/BETA, H_2-pretreated 1 wt% Ir/SSZ-13 and H_2-pretreated 1 wt% Ir/BETA catalysts.

Catalysts	State	Binding energy:Pt($4f_{7/2}$/$4f_{5/2}$) /eV, Pd($3d_{5/2}$/$3d_{3/2}$) /eV, Ir($4f_{7/2}$/$4f_{5/2}$) /eV	State	Binding energy: Pt ($4f_{7/2}$/$4f_{5/2}$) / eV, Pd($3d_{5/2}$/$3d_{3/2}$) /eV, Ir($4f_{7/2}$/$4f_{5/2}$) /eV	Fraction of two states/%
Pt/SSZ-13	Pt^0	70.6/74.4	Pt^{2+}	72.6/75.8	73.7/26.3
Pd/SSZ-13	Pd^{2+}	335.9/341.2	Pd^{4+}	338/343.4	21.2/78.9
Ir/SSZ-13	Ir^{3+}	62.1/65.0	Ir^{4+}	63.6/66.6	67.6/32.4
H_2-pre Ir/SSZ-13	Ir^0	61.0/64.0	Ir^{3+}	62.0/65.0	32.5/67.5
Ir/BETA	Ir^{3+}	62.3/65.4	Ir^{4+}	63.5/66.5	72.5/27.5
H_2-pre Ir/BETA	Ir^0	61.3/64.5	Ir^{3+}	62.3/65.3	50.2/49.8

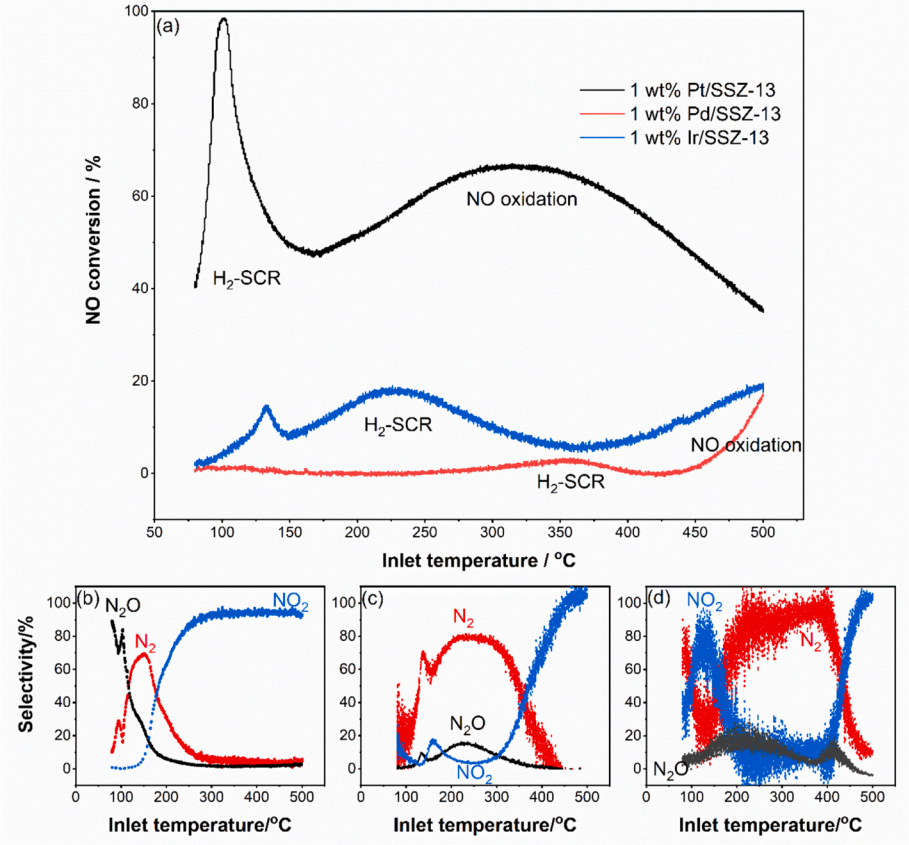

Fig. 1. (a) NO conversion of de-greened 1 wt% Pt/SSZ-13, 1 wt% Pd/SSZ-13 and 1 wt% Ir/SSZ-13 de-greened samples. (b-d) Selectivity of de-greened 1 wt% Pt/SSZ-13, 1 wt% Pd/SSZ-13 and 1 wt% Ir/SSZ-13. N_2 is determined by mass balance using FTIR data. (GHSV = 20,000 h^{-1}(STP); gas inlet: 10% O_2, 5% H_2O, 500 ppm NO, 5000 ppm H_2 balanced in Ar; T: 80–500 °C; heating rate: 5 °C/min).

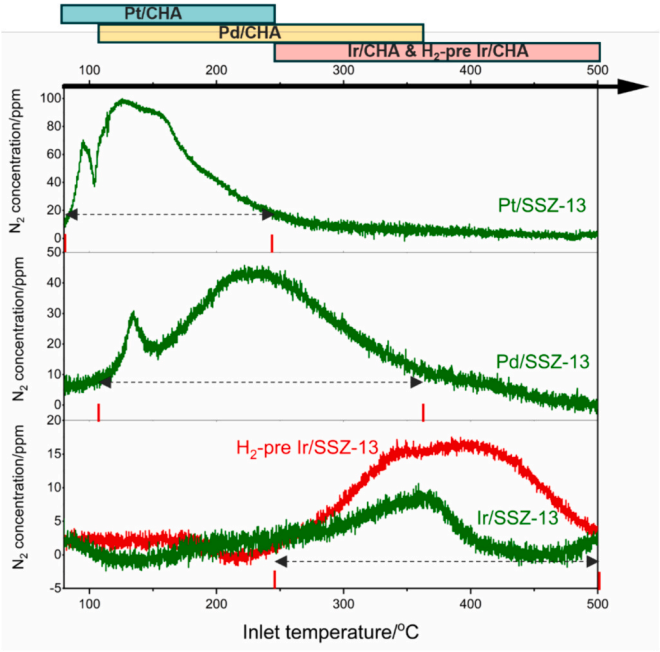

Fig. 2. Amounts and temperature intervals of N_2 generation on degreened 1 wt % Pt/SSZ-13, 1 wt% Pd/SSZ-13, 1 wt% Ir/SSZ-13 and H_2-pretreated 1 wt% Ir/SSZ-13.(GHSV = 20,000 h^{-1}(STP); gas inlet: 10% O_2, 5% H_2O, 500 ppm NO, 5000 ppm H_2 balanced in Ar; T: 80–500 °C; heating rate: 5 °C/min).

temperature range (**Fig. S2**), it is evident that there were some transient changes. The water production was shifted to higher temperature and eventually levels off resulting in the same water production for the oxidized and reduced sample (**Fig. S2(b)**). Interestingly, the nitrogen production (**Fig. S2(a)**) was similar in amount for the five cycles, but it shifted to somewhat higher temperatures. Thus, the nitrogen production capacity was maintained for the five cycles. The same reduction pretreatment strategy was also applied for the Pd/SSZ-13 sample but without any significant improvement (**Fig. S3**). In addition, the simultaneous increase in hydrogen feed concentration and the use of hydrogen pretreatment succeeded in increasing the overall activity for N_2 production of the three catalysts arranged in series (**Fig. S5**), indicating that the catalytic effect of the combination showed potential for further optimisation.

Besides the H_2-pretreatment strategy, Ir was loaded onto BETA zeolite instead of SSZ-13 chabazite zeolite with the same wet incipient impregnation method to further improve the activity of the Ir monometallic catalyst. It was observed in Fig. 3(b) that the H_2-pretreated BETA zeolite supported catalyst showed higher reactivity than the SSZ-13 supported catalyst. Moreover, after hydrogen pretreatment, nitrogen was generated at a lower and wider temperature range (140–450 °C), and the amount was nearly doubled. XPS results in Fig. 4 reveal that after hydrogen pretreatment, Ir^0 and Ir^{3+} were present instead of Ir^{3+} and Ir^{4+} both on the BETA and SSZ-13 supported catalysts along with specific values for the content of each state, as shown in Table 1. For the original oxygen-pretreated Ir/SSZ-13, two pairs of peaks are detected at the binding energy of 62.0/65.0 eV and 63.6/66.6 eV, which are assigned to $4f_{7/2}/4f_{5/2}$ of Ir^{3+} and Ir^{4+} species, respectively. After the reduction pretreatment, the two pairs of peaks appeared at lower binding energies at 61.0/64.0 eV and 62.0/65.0 eV, which belong to the

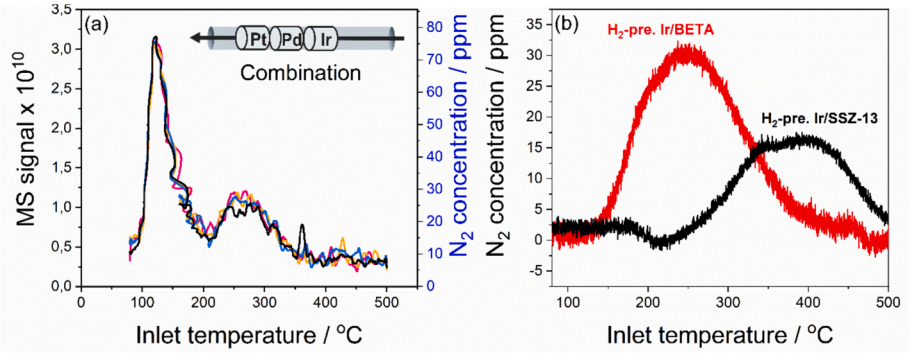

Fig. 3. (a) Mass spectrometry signals of N_2 generation and calibrated concentration (4 cycles) from the catalyst series: Ir/SSZ-13-Pd/SSZ-13-Pt/SSZ-13 (Pre-oxidized catalysts). (b) Comparison of activity results of H_2-pretreated Ir/BETA and Ir/SSZ-13 catalysts. (GHSV = 20,000 h^{-1}(STP); gas inlet: 10% O_2, 5% H_2O, 500 ppm NO, 5000 ppm H_2 balanced in Ar; T: 80–500 °C; heating rate: 5 °C/min).

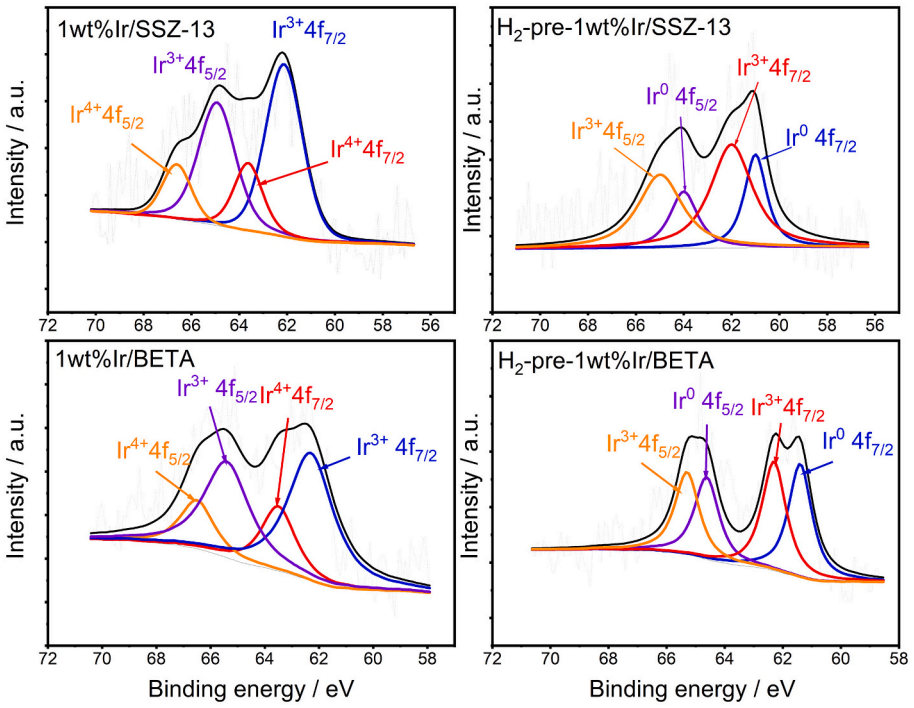

Fig. 4. XPS analysis results of 1 wt% Ir/SSZ-13 and 1 wt% Ir/BETA and their H_2-pretreated catalysts.

Ir^0 and Ir^{3+} species. It is also confirmed with the XPS data of BETA and SSZ-13 supported Ir catalysts, that H_2-pretreated Ir/BETA was in a more reduced state than Ir/SSZ-13, which is likely related to its higher activity for the H_2-SCR reaction.

DRIFT spectra were examined with de-greened 1 wt% Pt/SSZ-13, Pd/SSZ-13, and Ir/SSZ-13 samples to study aspects of the catalytic mechanism via a two-step procedure including NO adsorption and H_2-NO reaction. As is shown in Fig. 5(a), spectrums collected at 80 °C in 500 ppm NO gas flowing over the three catalysts have matching peaks at 2150, 1630, and 1590 cm^{-1}. It has been reported in several studies that the IR adsorption peak at 2150 cm^{-1} is assigned to NO_x species weakly adsorbed on the acidic sites of the zeolite [23]. The other two peaks appearing at 1630 and 1590 cm^{-1} belong to bridging nitrates and bidentate nitrates, respectively [24]. The intensities of these two peaks were relatively larger on the Ir/SSZ-13 catalyst, which illustrates that there was a stronger NO adsorption on Ir/SSZ-13 than on the Pd/SSZ-13 and Pt/SSZ-13 catalysts. Two additional IR peaks at 1860 and 1818 cm^{-1} were observed on the Pd/SSZ-13 catalyst, unlike the spectra of the Ir and Pt catalysts. In a recent study, Mandal and coworkers observed similar peaks during the adsorption of NO on Pd/SSZ-13 and suggested that the peak at 1860 cm^{-1} belongs to $Z[Pd^{II}(NO^-)(H_2O)_3]$, which was also comparable with the DFT-computed NO vibrational frequency [25]. Additionally, the peak at 1818 cm^{-1} has been attributed to $[ZPd^{I}(NO)]$ [26]. Briefly, the extra two peaks observed on Pd/SSZ-13 belong to NO adsorption on ion-exchanged Pd species. Considering the smaller particle size of the Pd catalyst, as shown in **Table S1,** compared to Pt/SSZ-13, it can be hypothesised that Pd probably was more ion-exchanged into the zeolite pores than Pt/SSZ-13. In fact, the similar two peaks were found on the surface of the other two catalysts, but with low intensities. NO and O_2 co-adsorption profiles were also studied and discussed in the **Supplementary Information** (**Fig. S6**). The NO adsorption spectra of de-greened Ir/SSZ-13 were recorded at an increased temperature of 200 °C (Fig. 5(b)). The peak at 1340 cm^{-1} had a dominant intensity and is assigned to a nitro complex on the metal cation of the metal oxide or nitrato species (NO_3^-) which could be formed by the surface O associated with NO [23,27,28]. The same peaks as for NO adsorption were also observed after flowing NO and H_2 simultaneously, suggesting that there was no or very limited H_2-SCR reaction.

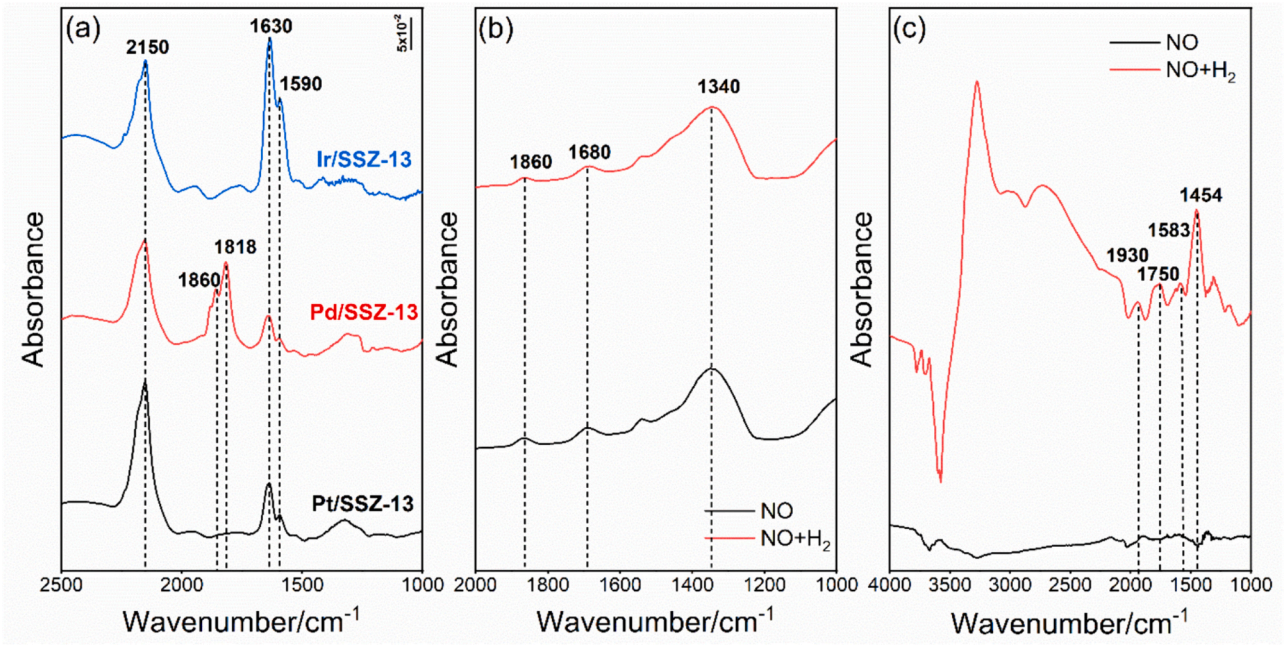

Fig. 5. In situ DRIFT spectra of (a) de-greened 1 wt% Pt/SSZ-13, Pd/SSZ-13, and Ir/SSZ-13 catalysts collected at 80 °C after exposure to 500 ppm NO; (b) de-greened 1 wt% Ir/SSZ-13 catalyst collected at 200 °C after exposure to 500 ppm NO (black) and 500 ppm NO +5000 ppm H_2 (red); (c) H_2-reduced 1 wt% Ir/SSZ-13 catalyst collected at 200 °C after exposure to 500 ppm NO (black) and 500 ppm NO +5000 ppm H_2 (red); All absorbance intensities in the spectrums are plotted in the same scale. (For interpretation of the references to colour in this figure legend, the reader is referred to the web version of this article.)

H_2-SCR will be hindered if NO is adsorbed on the catalyst in a highly stable state and cannot be catalytically decomposed for further reactions or because the overly strongly adsorbed NO occupies almost all active sites to the extent that H_2 cannot be adsorbed and dissociated into active atoms. The same NO adsorption measurements were done at 200 °C for Pt and Pd and the results did not show any characteristic peaks (**Fig. S7**). This suggests that the adsorption of NO_x on the surface of these two catalysts was not as stable at 200 °C.

Interestingly lr/SSZ-13 showed a weakened NO_x adsorption profile after being pre-reduced (black curve in Fig. 5(c) and **Fig. S8**. Although the 1340 cm^{-1} adsorption peak was still present in Fig. 5(c), significantly weaker adsorption on the reduced sample can be seen in **Fig. S8**. These results can explain the increased activity for NO and H_2 over the reduced Ir/SSZ-13. Many of the newly generated bands in the DRIFT measurements were likely linked to the reduced Ir catalyst promoting the catalytic activity as evident by the activity tests. Large peaks beyond 2000 cm^{-1} were mainly assigned to O—H stretching from water formation which is the main product of the reaction [29]. The other smaller peaks at 1750 and 1930 cm^{-1} are related to H_2O adsorption on the zeolite framework or nitrates adsorbed on the support [30–32]. The peak at 1454 cm^{-1} indicates the formation of ammonium ions on the catalyst which plays a role as an intermediate in the reaction process [33].

4. Conclusion

In conclusion, the three metals – Pt, Pd, and Ir supported on SSZ-13 zeolite were evaluated for H_2-SCR activity and proven to have their distinct functional temperature intervals covering a broad temperature range for the reduction of NO to N_2. Since Ir has a special high-temperature activity for H_2-SCR, reduction pretreatment, as well as its loading on a different support, namely BETA zeolite, were two strategies that could be used to improve its performance. DRIFT measurements demonstrated (i) strong NO adsorption on the de-greened Ir/SSZ-13 catalyst at 80 °C (ii) Pd was present to a greater extent as ion-exchange ions compared to the other two metals (iii) oxidatively-pretreated Ir/SSZ-13 adsorbed NO_x in a different state and was more stable at 200 °C (iv) after reduction treatment, NO_x adsorption on the surface of Ir at 200 °C was weakened, which contributed to the subsequent reaction.

CRediT authorship contribution statement

Jieling Shao: Investigation, Formal analysis, Visualization, Writing – original draft. **Phuoc Hoang Ho:** Supervision, Writing – review & editing. **Derek Creaser:** Supervision, Writing – review & editing. **Louise Olsson:** Funding acquisition, Resources, Supervision, Writing – review & editing.

Declaration of competing interest

The authors declare that they have no known competing financial interests or personal relationships that could have appeared to influence the work reported in this paper.

Data availability

Data will be made available on request.

Acknowledgements

The authors acknowledge the funding by the Swedish Energy Agency and the collaboration with Volvo AB, Scania CV, and Johnson Matthey via a Strategic Vehicle Research and Innovation (FFI) project (P51458-1).

Appendix A. Supplementary data

Supplementary Information to this article can be found online at https://doi.org/10.1016/j.apcato.2024.206947.

References

[1] S.A. Neves, A.C. Marques, M. Patrício, Determinants of CO2 emissions in European Union countries: does environmental regulation reduce environmental pollution? Econ. Anal. Policy 68 (2020) 114–125, https://doi.org/10.1016/j.eap.2020.09.005.

[2] L. Rouleau, F. Duffour, B. Walter, R. Kumar, L. Nowak, Experimental and Numerical Investigation on Hydrogen Internal Combustion Engine, 2021, https://doi.org/10.4271/2021-24-0060.

[3] M.R. Swain, J.M. Pappas, R.R. Adt, W.J.D. Escher, Hydrogen-Fueled Automotive Engine Experimental Testing to Provide an Initial Design-Data Base, 2018.

[4] Z. Liu, J. Li, S.I. Woo, Recent advances in the selective catalytic reduction of NOx by hydrogen in the presence of oxygen, Energy Environ. Sci. 5 (2012) 8799–8814, https://doi.org/10.1039/c2ee22190j.

[5] M. Machida, K. Nishiyama, M. Furukubo, H. Yoshida, K. Awaya, J. Ohyama, M. Tsushida, M. Suwa, Y. Nagao, Y. Endo, T. Wakabayashi, Pt oxide nanoclusters supported on ZrP2O7 for selective NOx reduction by H2 in the presence of O2 with negligible NH3, N2O, and NO2 byproducts, ACS Appl. Nano Mater. 7 (2024) 766–776, https://doi.org/10.1021/acsanm.3c04898.

[6] Y. Zhang, S. Xu, Y. Wang, Z. Liu, Selective catalytic reduction of NOx by H2 over Na modified Pd/TiO2 catalyst, Int. J. Hydrog. Energy 48 (2023) 16267–16278, https://doi.org/10.1016/j.ijhydene.2023.01.099.

[7] J. Shibata, M. Hashimoto, K.I. Shimizu, H. Yoshida, T. Hattori, A. Satsuma, Factors controlling activity and selectivity for SCR of NO by hydrogen over supported platinum catalysts, J. Phys. Chem. B 108 (2004) 18327–18335, https://doi.org/10.1021/jp046705v.

[8] R. Burch, M.D. Coleman, An Investigation of the NO/H 2 /O 2 Reaction on Noble-Metal Catalysts at Low Temperatures under Lean-Burn Conditions, 1999.

[9] M. Engelmann-Pirez, P. Granger, G. Leclercq, Investigation of the catalytic performances of supported noble metal based catalysts in the NO + H2 reaction under lean conditions, Catal. Today (2005) 315–322, https://doi.org/10.1016/j.cattod.2005.07.087.

[10] Z.P. Liu, S.J. Jenkins, D.A. King, Step-enhanced selectivity of NO reduction on platinum-group metals, J. Am. Chem. Soc. 125 (2003) 14660–14661, https://doi.org/10.1021/ja0372208.

[11] H. Shinjoh, Noble metal sintering suppression technology in three-way catalyst: automotive three-way catalysts with the noble metal sintering suppression technology based on the support anchoring effect, Catal. Surv. Jpn. 13 (2009) 184–190, https://doi.org/10.1007/s10563-009-9076-6.

[12] J. Kim, J. Yu, S. Lee, A. Tahmasebi, C.H. Jeon, J. Lucas, Advances in catalytic hydrogen combustion research: catalysts, mechanism, kinetics, and reactor designs, Int. J. Hydrog. Energy 46 (2021) 40073–40104, https://doi.org/10.1016/j.ijhydene.2021.09.236.

[13] J.F. Kramer, S.-A.S. Reihani, G.S. Jackson, Low-Temperature Combustion of Hydrogen on Supported PD Catalysts, 2002.

[14] X. Li, X. Zhang, Y. Xu, Y. Liu, X. Wang, Influence of support properties on H2 selective catalytic reduction activities and N2 selectivities of Pt catalysts, Cuihua Xuebao/Chinese, J. Catal. 36 (2015) 197–203, https://doi.org/10.1016/S1872-2067(14)60197-2.

[15] B. Wen, NO Reduction with H2 in the Presence of Excess O2 over Pd/MFI Catalyst Q. www.fuelfirst.com, 2024.

[16] M. Borchers, P. Lott, O. Deutschmann, Selective catalytic reduction with hydrogen for exhaust gas after-treatment of hydrogen combustion engines, Top. Catal. 66 (2023) 973–984, https://doi.org/10.1007/s11244-022-01723-1.

[17] A.M. Beale, F. Gao, I. Lezcano-Gonzalez, C.H.F. Peden, J. Szanyi, Recent advances in automotive catalysis for NOx emission control by small-pore microporous materials, Chem. Soc. Rev. 44 (2015) 7371–7405, https://doi.org/10.1039/c5cs00108k.

[18] F. Gao, J. Szanyi, On the hydrothermal stability of Cu/SSZ-13 SCR catalysts, Appl. Catal. A Gen. 560 (2018) 185–194, https://doi.org/10.1016/j.apcata.2018.04.040.

[19] Z. Hong, X. Sun, Z. Wang, G. Zhao, X. Li, Z. Zhu, Pt/SSZ-13 as an efficient catalyst for the selective catalytic reduction of NO: X with H2, Catal. Sci. Technol. 9 (2019) 3994–4001, https://doi.org/10.1039/c9cy00898e.

[20] T. Nanba, C. Kohno, S. Masukawa, J. Uchisawa, N. Nakayama, A. Obuchi, Improvements in the N2 selectivity of Pt catalysts in the NO-H2-O2 reaction at low temperatures, Appl. Catal. B 46 (2003) 353–364, https://doi.org/10.1016/S0926-3373(03)00227-3.

[21] A. Cybulski, J. Moulin, Monoliths in heterogeneous catalysis, Catal. Rev. 36 (1994) 179–270, https://doi.org/10.1080/01614949408013925.

[22] T. Li, M. Kim, Z. Liang, A. Asthagiri, J.F. Weaver, Hydrogen oxidation on oxygen-rich IrO2(110), Catalys. Struct. Reactiv. 4 (2018) 1–13, https://doi.org/10.1080/2055074X.2018.1565002.

[23] P.G. Savva, A.M. Efstathiou, The influence of reaction temperature on the chemical structure and surface concentration of active NOx in H2-SCR over Pt/MgO{single bond}CeO2: SSITKA-DRIFTS and transient mass spectrometry studies, J. Catal. 257 (2008) 324–333, https://doi.org/10.1016/j.jcat.2008.05.010.

[24] C.N. Costa, A.M. Efstathiou, Transient isotopic kinetic study of the NO/H2/O2 (lean de-NOx) reaction on Pt/SiO2 and Pt/La-Ce-Mn-O catalysts, J. Phys. Chem. B 108 (2004) 2620–2630, https://doi.org/10.1021/jp030934k.

[25] K. Mandal, Y. Gu, K.S. Westendorff, S. Li, J.A. Pihl, L.C. Grabow, W.S. Epling, C. Paolucci, Condition-dependent Pd speciation and NO adsorption in Pd/zeolites, ACS Catal. 10 (2020) 12801–12818, https://doi.org/10.1021/acscatal.0c03585.

[26] K. Khivantsev, N.R. Jaegers, L. Kovarik, J.C. Hanson, F. Feng Tao, Y. Tang, X. Zhang, I.Z. Koleva, H.A. Aleksandrov, G.N. Vayssilov, Y. Wang, F. Gao, J. Szanyi, Achieving atomic dispersion of highly loaded transition metals in Small-Pore Zeolite SSZ-13: high-capacity and high-efficiency low-temperature CO and passive NO x adsorbers, Angew. Chem. 130 (2018) 16914–16919, https://doi.org/10.1002/ange.201809343.

[27] E. Ito, Y.J. Mergler, B.E. Nieuwenhuys, H.P.A. Calk, H. Van Bekkum, C.M. Van Den Bleek, IR Mechanistic Studies on NO Reduction with NH3 in the Presence of Oxygen over Cerium-Exchanged Mordenite, 1996.

[28] K. Nakamoto, Infrared and Raman Spectra of Inorganic and Coordination Compounds, Wiley, 2008, https://doi.org/10.1002/9780470405888.

[29] J. Lengyel, M. Ončák, A. Herburger, C. Van Der Linde, M.K. Beyer, Infrared spectroscopy of O- and OH- in water clusters: evidence for fast interconversion between O- and OHOH, Phys. Chem. Chem. Phys. 19 (2017) 25346–25351, https://doi.org/10.1039/c7cp04577h.

[30] C.N. Costa, A.M. Efstathiou, Mechanistic aspects of the H2-SCR of NO on a Novel Pt/MgO-CeO2 catalyst, J. Phys. Chem. C 111 (2007) 3010–3020, https://doi.org/10.1021/jp064952o.

[31] H. Jobic, M. Czjzek, R.A. van Santen, Interaction of Water with Hydroxyl Groups in H-Mordenite: A Neutron Inelastic Scattering Study, Heyden: London. https://pubs.acs.org/sharingguidelines, 1992.

[32] H.A. Al-Abadleh, V.H. Grassian, FT-IR study of water adsorption on aluminum oxide surfaces, Langmuir 19 (2003) 341–347, https://doi.org/10.1021/la026208a.

[33] L. Čapek, K. Novoveská, Z. Sobalík, B. Wichterlová, L. Cider, E. Jobson, Cu-ZSM-5 zeolite highly active in reduction of NO with decane under water vapor presence: comparison of decane, propane and propene by in situ FTIR, Appl. Catal. B 60 (2005) 201–210, https://doi.org/10.1016/j.apcatb.2005.02.033.